Sensor systems

A Three-Dimensional Integrated Micro Calorimetric Flow Sensor in CMOS MEMS Technology

Wei Xu[1,2], Bo Wang[3], Mingzheng Duan[2], Moaaz Ahmed[3], Amine Bermak[2,3*], and Yi-Kuen Lee[2]

[1]College of Electronic Science and Technology, Shenzhen University, Shenzhen 518000, China
[2]Department of Mechanical and Aerospace Engineering, Hong Kong University of Science and Technology, Hong Kong
[3]Division of Information and Computing Technology, College of Science and Engineering, Hamad Bin Khalifa University, 34110, Doha, Qatar
*Fellow, IEEE

Manuscript received January 2, 2019; accepted January 13, 2019. Date of publication January 16, 2019; date of current version February 6, 2019.

Abstract—This article presents a 3-D integrated molybdenum (Mo) thermoresistive microcalorimetric flow sensor in a 0.18-μm CMOS MEMS technology. The sensor consists of a MEMS structure which is fabricated inside a sealed microchannel and a constant temperature control circuit implemented on the CMOS wafer. The MEMS structure and the CMOS circuit are 3-D integrated at the wafer level. For the N_2 gas flow, the proposed flow sensor achieves a high sensitivity of 0.71 mV/(m/s) and a wide bidirectional detection ability of −26–26 m/s. Moreover, an equivalent circuit model is proposed in this article, which depicts the nonlinear output/overheated temperature ($V_{out}/\Delta T_h$) sensor response to the input gas flow. This model would be an efficient tool for the design and optimization of high-performance system-on-chip calorimetric flow sensors.

Index Terms—Sensor systems, calorimetric flow sensor, CMOS MEMS, microchannel, thermoresistive, 3-D integration.

I. INTRODUCTION

Flow measurements are amenable to a wide variety of physical principles [1]. As one type of flow devices, the thermal-based flow sensors with no moving parts and good CMOS compatibilities have attracted great research interests in recent years [2]–[7]. However, most previously reported sensors require costly packaging to achieve reliable flow sensing, such as the flip chip packaging [8]–[10]; the surface mounted adaptor with the flow channel on the chip [11], [12]; and the sealed flow channel with the sensor chip [13] or a part of sensor chip inside [14]. To the best of our knowledge [15], [16], very few 3-D CMOS MEMS thermal flow sensors [17] have been reported with the system-on-chip (SoC) solution. Herein, 3-D means the sensor was integrated into a self-packaged microchannel formed between a CMOS die and a MEMS die (see Fig. 1).

The microcalorimetric flow sensor is one of the heat-convection based measurement devices that monitor the flow-induced asymmetric temperature profile around the microheater. As shown in Fig. 1, with a symmetrical arrangement, temperature difference ΔT between the upstream and the downstream thermistors solely reflects the forced heat convection, while the sensor sensitivity and accuracy can be significantly improved, especially for small input flow [18], [19].

Two operation modes are usually used in microcalorimetric flow sensors: one is to drive the microheater with a constant current (CC) or voltage (CV). Another method is to employ a feedback circuit to keep the microheater under constant temperature (CT) condition [20], [21]. Despite the complexity of implementation, the CT operation mode provides better sensing resolution, wider detection range, and faster dynamic response than those of CC or CV mode [17], [22], [23]. Previously, we reported a CMOS MEMS flow sensor which demon-

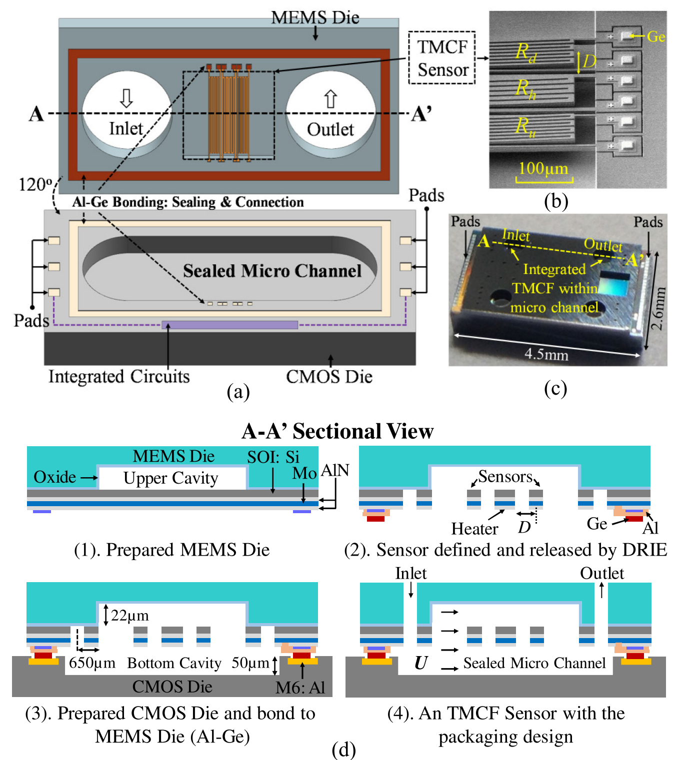

Fig. 1. (a) Schematic of a 3-D integrated CMOS TMCF sensor within an internal micro flow channel by using the proprietary 0.18-μm InvenSense CMOS MEMS process. (b) SEM micrograph of TMCF sensor with the serpentine structure. (c) Optical view of the fabricated 3-D integrated TMCF sensor die. (d) Key fabrication steps of the 3-D integrated flow sensor.

Corresponding author: Wei Xu (e-mail: weixu@szu.edu.cn).
Associate Editor: Y. Suzuki.
Digital Object Identifier 10.1109/LSENS.2019.2893151

1949-307X © 2019 IEEE. Personal use is permitted, but republication/redistribution requires IEEE permission.
See http://www.ieee.org/publications_standards/publications/rights/index.html for more information.

strated a unidirectional flow range with a one-way CFIA based readout circuit [24]. However, a bulky off-chip CT mode-based microheater feedback circuit is needed to enable its operation.

In this letter, a new 3-D integrated CMOS MEMS flow sensor with an on-chip interface circuit (includes a CT mode-based feedback circuit and a Wheatstone bridge-based readout circuit) was designed, fabricated, and characterized. The first contribution of this article is from the SoC design and fabrication perspective, whereby a very compact and self-packaged flow sensor is presented. Different from the monolithically integrated design [25], this CMOS MEMS flow sensor with the integrated microchannel and the interface circuit can significantly reduce the cumbersome packaging costs required for flow measurement. Second, we also proposed an analytical 1-D model that can better characterize the nonlinear heat transfer phenomenon of the CMOS calorimetric flow sensor and an equivalent circuit model (ECM) that can depict the coupled electro-thermal-mechanical effect on the sensor system performance. These models would be effective tools for the design and optimization of high-performance SoC calorimetric flow sensors.

II. DESIGN OF CMOS THERMORESISTIVE MICROCALORIMETRIC FLOW (TMCF) SENSOR

A. TMCF Sensor

As shown in Fig. 1, the proposed TMCF sensor consists of one centered molybdenum (Mo) microheater (R_h) and two symmetrically placed Mo thermoresistive sensors (R_u and R_d) on a 5-μm-thick silicon-based suspended microbridge structure. The TMCF sensor was fabricated in a proprietary InvenSense 0.18-μm CMOS MEMS process [26], where the sensor is wafer-level sealed with an SOI MEMS wafer bonded to a 0.18-μm CMOS wafer. The detailed fabrication process of Mo TMCF sensor can be found elsewhere [17]. The micrograph of the fabricated MEMS sensor on a 400 μm × 400 μm × 22 μm (length × width × height) upper cavity is shown in Fig. 1(b), where the flow sensor is integrated into a 3-D stacked structure [see Fig. 1(c)] with the sealed microflow channel (length × width × height: 2200 μm × 400 μm × 50 μm). To realize the integrated flow channel with the cost reduction of packaging, circular fluids inlet and outlet with a diameter of 510 μm were opened on the MEMS wafer, as shown in Fig. 1(d).

Previously, we reported a general 1-D model to predict the characteristics of a CMOS TMCF sensor by considering the boundary layer effect on one side of the flow sensor [25]. In this SoC design, the double-sided fluids flow over the MEMS sensor, as validated by the computational fluid dynamics (CFD) study [18], was sensed. Therefore, with the assumptions of a uniform flow profile U and the upper and the bottom thermal boundary thickness equal to cavity heights, a new 1-D analytical model with the considered double-sided flow in (1), shown below, is proposed to design the 3-D integrated flow sensor

$$k_f(h_u + 2t + h_d)\frac{d^2T(x)}{dx^2} - \rho C_P U \frac{dT(x)}{dx}(h_u + 2t + h_d) - k_f\left(\frac{2}{h_u} + \frac{2}{h_d}\right)T(x) = 0 \quad (1)$$

where h_u and h_d are the upper and bottom cavity heights; t is the sensor thickness; and k_f, ρ, and C_p are the thermal conductivity, density, and heat capacity of the moving fluid, respectively.

Good agreement of thermal output ΔT between the 1-D model (a fitting factor ε of 2.7) and the validated CFD study [18] is observed in Fig. 2(a), which demonstrates that this 1-D model can effectively predict the sensor response and significantly speed up the sensor design. As shown in Fig. 2(b), the 1-D model analysis shows that the TMCF sensor can achieve the highest sensitivity S with the distance between microheater and thermistors $D \approx 30$ μm for small input flow velocity. To comply with the design rule of the CMOS MEMS process [26], the distance D is designed to be 32 μm.

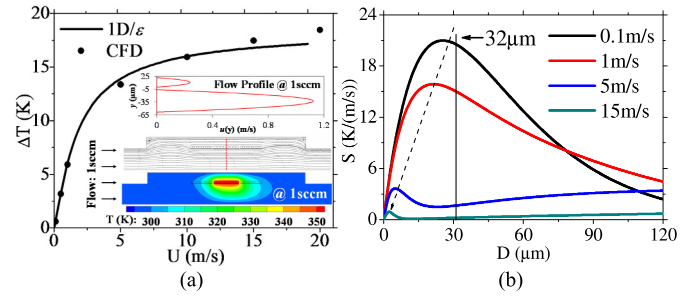

Fig. 2. (a) Comparison of the sensor output between CFD and 1-D model. (b) Effect of distance D between the heater and sensing elements on the TMCF sensor's sensitivity, where an optimal distance $D = 32$ μm was determined.

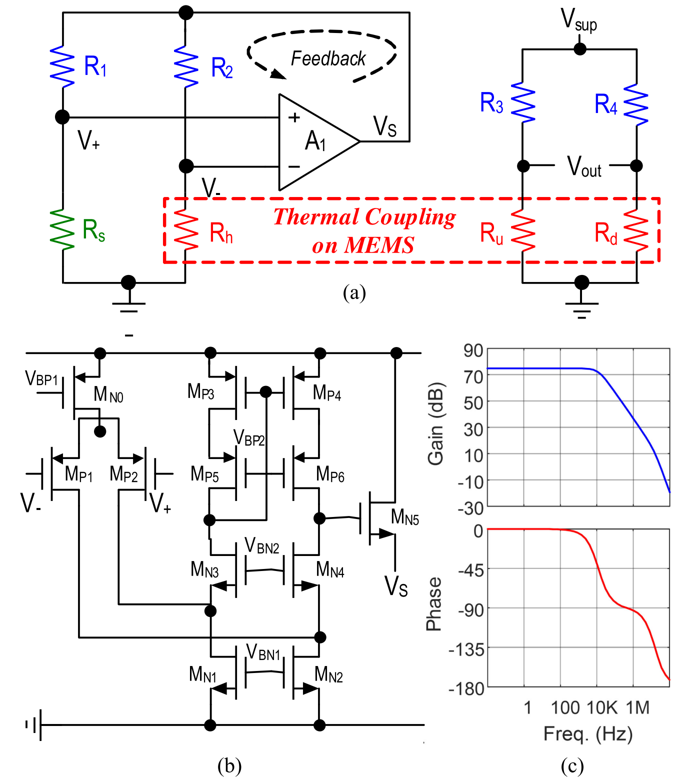

Fig. 3. Proposed on-chip interface circuit for CMOS TMCF sensor. (a) Microheater control circuit. (b) Folded-cascode amplifier with an NMOS buffer stage. (c) Simulated open-loop gain and phase of the CT control circuit.

B. Interface Circuits

Besides the MEMS design, an integrated CMOS interface circuit is implemented on the CMOS die [see Fig. 1(a)] to realize a tangible SoC TMCF solution. As shown in Fig. 3(a), R_h, R_u, and R_d are the microheater and thermoresistive sensors in the MEMS structure, respectively; R_1 and R_2 are on-chip polysilicon resistors; and R_3 and

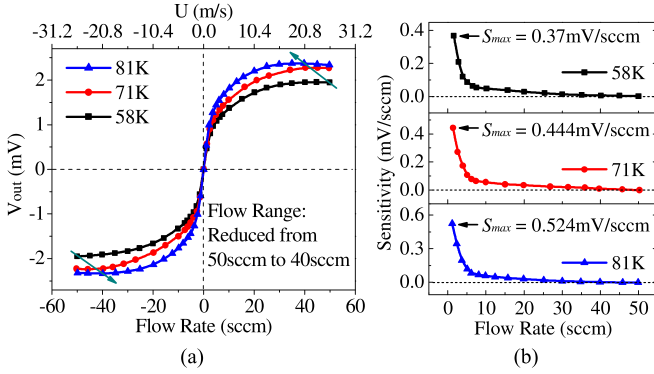

Fig. 4. CT operated TMCF sensor (a) output and (b) sensitivity response to the nitrogen flow −50–50 sccm (−26–26 m/s).

R_4 are on-chip Mo resistors, while R_s is an off-chip resistor. During the operation, the negative feedback loop around an operational amplifier A_1 guarantees $V_+ = V_-$. Therefore, with $R_1 = R_2 = 76\ \Omega$, $R_h = R_s$ will hold under different input gas flows, which ensures the CT operation of R_h. With a temperature coefficient of microheater $\alpha = 2.22 \times 10^{-3}$ and $R_s = 343\ \Omega$, the resistance of the microheater ($R_h = 304\ \Omega$ @ 22 °C) will be increased by the joule heating until the CT circuit is balanced, where a constant temperature $T_h = 80$ °C ($\Delta T_h = T_h$ - T_a = 58 K) on R_h should be maintained. The reason to choose $\Delta T_h = 58$ K is to minimize the heating power of microheater (<13 mW), while without heavily degrading the output signal strength. Moreover, under this condition, the required voltage on the microheater $V_h < 2.1$ V, which enables the SoC system to be operated with a single 5 V supply. With the thermal coupling of the MEMS sensor in the CT operation mode, the thermal difference output ΔT between R_u and R_d can be converted to a voltage output V_{out} by using an on-chip Wheatstone bridge formed with R_3, R_4, R_u, and R_d.

For the detailed CT circuit, a folded-cascade amplifier with a gain $A = 75$ dB is designed in Fig. 3(b). A large input transistor of 500 μm × 0.35 μm and an overdrive voltage of 0.35 V are used to improve the device matching and ensure an offset V_{off} <2 mV for accurate CT control. Meanwhile, an NMOS buffer M_{N5} is added to isolate the gain stage and drive 210 Ω resistive load formed by R_1, R_2, R_s, and R_h. The driving ability of this amplifier is designed to be 16 mA, which allows a maximum sensible flow of 26 m/s without the significant drops of microheater temperature. Fig. 3(c) shows the simulated loop gain and phase of the CT control circuit. The overall power consumption of this amplifier is 95 μW @ 5 V, which ensures most of the system power is consumed by the heating elements and the output stage.

III. RESULTS AND DISCUSSION

The measured output of the TMCF sensor is plotted against the N_2 gas flow from −50 to 50 sccm (−26–26 m/s), as shown in Fig. 4(a). The TMCF sensor is capable of detecting the bidirectional fluids flow. Meanwhile, the sensitivity of the TMCF sensor that defined as the slope of linear fit between two calibrated data points is plotted in Fig. 4(b). The proposed SoC sensor shows a high sensitivity of 0.37 mV/sccm [0.71 mV/(m/s)] and a large flow range of −50–50 sccm (−26–26 m/s) in a CT mode (T_h = 80 K and ΔT_h = 58 K). As shown in Table 1, the normalized sensitivity (57 μV/(m/s)/mW) with respect to the input heating power is better than those CMOS flow sensors in the literature [11], [27] and shows comparable performance with the monolithically released CMOS sensor [25]. More-

TABLE 1. Comparison Between the Previous CMOS Flow Sensor and Current Work.

References	DS, mm^2	Packaging	F	FR, m/s	P, mW	S^*, µV/(m/s)/mW
Wu [8]	16	Flip to Ceramic	Air	1~25	25	N/A
Bruschi [11]	16	PMMA adaptor	N_2	-3.33~3.33	4	23
Xu [25]	2.25	PMMA Channel	N_2	-11~11	2.36~2.77	154.4
Dong [27]	36	Flip to Ceramic	Air	0.5~40	2~452.6	39.3
Our work	**3.4**	**Self-packaged**	**N_2**	**-26~26**	**12.2~16.7**	**58.2**

DS = Device Size; *F* = Fluids; *FR* = Flow Range; *P* = Power; S^* = Sensitivity normalized with respect to input power and gain.

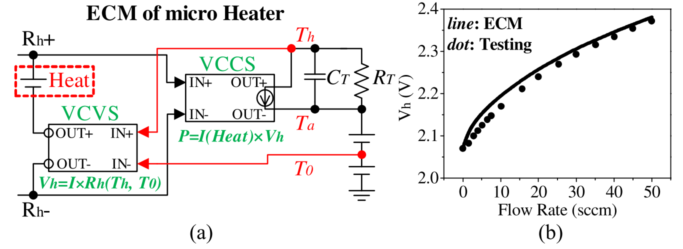

Fig. 5. (a) ECM of the TCMF sensor's microheater. (b) Comparison of ECM simulation with experimental results.

over, the proposed flow sensor achieves the best bidirectional detection range of −26–26 m/s. It is worth mentioning that the proposed sensor design has a much more compact feature size thanks to the self-integrated microflow channel, while it can cut down the costly and bulk sensor packaging as compared to the monolithically integrated one [25].

To obtain a higher output/sensitivity SoC flow device, more input heating power can be consumed with the increased ΔT_h [19]. Obviously, with the microheater work in ΔT_h = 71 K and 81 K (see Fig. 4), the sensitivity can be further improved to 0.444 mV/sccm and 0.524 mV/sccm, respectively. However, different from the previously observed linear behavior of $V_{\text{out}}/\Delta T_h$ [19], the flow range of this SoC device is reduced from −50–50 sccm to −40–40 sccm with the increased heating power. The reason behind this discrepancy could be explained by an ECM simulation with the investigated electro-thermal-mechanical coupling phenomena of the microheater.

Based on the energy balance described by a modified King's law [28], the ECM of the microheater [see Fig. 5(a)] is expressed by a thermal capacitance C_T and a thermal resistance R_T [29]. As shown in Fig. 5(b), the ECM successfully captures the microheater output response V_h, where the simulated results are in good agreement with the testing data with an error of < 1.5%. From the ECM simulation, the SoC flow sensor working in ΔT_h = 58 K shows a 6 K decline of ΔT_h when the flow goes to 50 sccm [see Fig. 6(b)]. The decline of ΔT_h is due to the small system loop gain of gR_BA, as shown in the following equation [30]:

$$I_h = \frac{gR_B A V_{\text{off}}(R_1 + R_s)}{(R_1 + R_s)(R_2 + R_h) + gR_B A(R_1 R_h - R_2 R_s)} \quad (2)$$

where $gR_B < 1$, g is the conductance of NMOS, and R_B is the loading resistance formed by R_1, R_2, R_s, and R_h. When the convective flow increase, the increment of feedback current I_h is not large enough to power up R_h with the maintained constant ΔT_h. Besides, the flow range was further reduced due to the CT-based sensor system (ΔT_h = 81 K) toward saturation [see the V_h response in Fig. 6(a)], while a 14.3 K decline of ΔT_h is observed. To ensure much more accurately

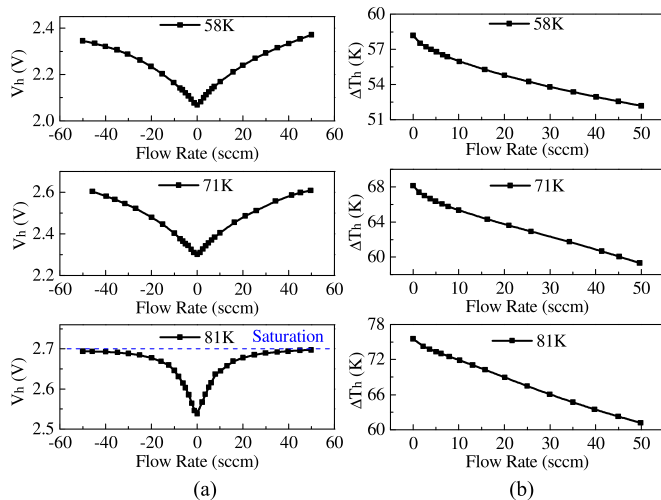

Fig. 6. (a) Measured microheater voltage response and (b) ECM simulated ΔT_h of the SoC flow sensor under different configured working temperatures.

controlled CT mode for the SoC flow sensor with the good flow range and high sensitivity, future work will consider designing a larger gain based operational transconductance amplifier with a stronger current buffer (larger g).

IV. CONCLUSION

We reported a 3-D integrated TMCF sensor with the suspended sensor structure inside a wafer-level sealed microchannel by using CMOS MEMS Technology. For the N_2 gas flow, the SoC device that configured with a specialized on-chip CT circuit achieves a good sensitivity of 0.71 mV/(m/s) with the bidirectional detection ability of −26–26 m/s. Besides, the nonlinear $V_{\text{out}}/\Delta T_h$ response of the SoC TMCF sensor is depicted by an ECM model, which would be a powerful mean for the design and optimization of CMOS TMCF sensors. With the SoC solution, this proposed low-cost TMCF sensor will be a promising flow device for the Internet of things.

ACKNOWLEDGMENT

The authors would like to thank W. L. Yeung for technical support, as well as the staff at HKUST NFF and MCPF. This work was supported by the Hong Kong ITF Grant (ITS/410/16FP) via HKUST-MIT Research Consortium, Guangzhou Science, Technology and Innovation Commission (201704030101) and Guangdong Science and Technology Grant (2017B050506001).

REFERENCES

[1] N. Nguyen, “Micromachined flow sensors—A review,” *Flow Meas. Instrum.*, vol. 8, pp. 7–16, 1997.

[2] Y. Wang *et al.*, “MEMS-based gas flow sensors,” *Microfluid. Nanofluid.*, vol. 6, pp. 333–346, 2009.

[3] J. T. Kuo, L. Yu, and E. Meng, “Micromachined thermal flow sensors—A review,” *Micromachines*, vol. 3, pp. 550–573, 2012.

[4] S. Silvestri and E. Schena, “Micromachined flow sensors in biomedical applications,” *Micromachines*, vol. 3, pp. 225–243, 2012, doi: 10.3390/mi3020225.

[5] W. Fang *et al.*, “CMOS MEMS: A key technology towards the “More than Moore” era,” in *Proc. IEEE Transducers Eurosensors XXVII*, Barcelona, Spain, 2013, pp. 2513–2518.

[6] A. De Luca and F. Udrea, “CMOS MEMS hot-film thermoelectronic flow sensor,” *IEEE Sensors Lett.*, vol. 1, no. 6, pp. 1–4, Dec. 2017.

[7] H. Baltes, O. Paul, and O. Brand, “Micromachined thermally based CMOS microsensors,” *Proc. IEEE*, vol. 86, no. 8, pp. 1660–1678, Aug. 1998.

[8] J. Wu, C. van Vroonhoven, Y. Chae, and K. Makinwa, “A 25mW CMOS sensor for wind and temperature measurement,” in *Proc. IEEE Sensors*, Limerick, Ireland, Oct. 28–31, 2011, pp. 1261–1264.

[9] J.-B. Sun, M. Qin, and Q.-A. Huang, “A flip-chip packaged CMOS thermal flow sensor,” in *Proc. IEEE Sensors*, Irvine, CA, USA, 2005, pp. 557–560.

[10] F. Mayer, O. Paul, and H. Baltes, “Flip-chip packaging for thermal CMOS anemometers,” in *Proc. IEEE 10th Annu. Int. Workshop Micro Electro Mech. Syst. Investigation Micro Struct., Sensors, Actuators, Mach. Robots*, Nagoya, Japan, 1997, pp. 203–208.

[11] P. Bruschi, M. Dei, and M. Piotto, “A single chip, double channel thermal flow meter,” *Microsyst. Technol.*, vol. 15, pp. 1179–1186, 2009.

[12] P. Bruschi, M. Dei, and M. Piotto, “An offset compensation method with low residual drift for integrated thermal flow sensors,” *IEEE Sensors J.*, vol. 11, no. 5, pp. 1162–1168, May 2011.

[13] W. Xu, L. Pan, B. Gao, Y. Chiu, K. Xu, and Y.-K. Lee, “Systematic study of packaging designs on the performance of CMOS thermoresistive micro calorimetric flow sensors,” *J. Micromech. Microeng.*, vol. 27, no. 8, Jun 2017, Art. no. 085001.

[14] G. Dumstorff, E. Brauns, and W. Lang, “Investigations into packaging technology for membrane-based thermal flow sensors,” *J. Sens. Sens. Syst.*, vol. 4, pp. 45–52, 2015.

[15] A. C. Fischer *et al.*, “Integrating MEMS and ICs,” *Microsyst. Nanoeng.*, vol. 1, 2015, Art. no. 15005.

[16] H. Qu, “CMOS MEMS fabrication technologies and devices,” *Micromachines*, vol. 7, no. 1, 2016, Art. no. 14.

[17] W. Xu *et al.*, “A wafer-level encapsulated CMOS MEMS thermoresistive calorimetric flow sensor with integrated packaging design,” in *Proc. IEEE Int. Conf. Micro Electro Mech. Syst.*, Las Vegas, 2017, pp. 989–992.

[18] B. Lijin, W. Xu, M. Paszkiewicz, Z. Li, R. Wang, and Y. K. Lee, “Theoretical and experimental study of peclet number effect on the linearity of thermoresistive micro calorimetric flow sensors,” in *Proc. 9th Asia-Pac. Conf. Transducers Micro-Nano Technol.*, Hong Kong, Jun. 2018.

[19] W. Xu, B. Gao, S. Ma, A. Zhang, Y. Chiu, and Y. K. Lee, “Low-cost temperature-compensated thermoresistive micro calorimetric flow (T2MCF) sensor by using 0.35μm CMOS MEMS technology,” in *Proc. IEEE 29th Int. Conf. Micro Electro Mech. Syst.*, Shanghai, China, Jan. 24–28, 2016, pp. 189–192.

[20] G. C. Lomas, *Fundamentals of Hot Wire Anemometry*. Cambridge, U.K.: Cambridge Univ. Press, 2011.

[21] A. E. Perry, *Hot-Wire Anemometry*. Oxford, U.K.: Clarendon, 1982.

[22] C. Sosna, T. Walter, and W. Lang, “Response time of thermal flow sensors with air as fluid,” *Sens. Actuator A, Phys.*, vol. 172, pp. 15–20, 2011.

[23] R.Vilares *et al.*, “Fabrication and testing of a SU-8 thermal flow sensor,” *Sens. Actuator B, Chem.*, vol. 147, no. 2, pp. 411–417, 2010.

[24] M. Ahmed, W. Xu, S. Mohamad, M. Duan, Y. Lee, and A. Bermak, “Integrated CMOS-MEMS flow sensor with high sensitivity and large flow range,” *IEEE Sensors J.*, vol. 17, no. 8, pp. 2318–2319, Apr. 2017.

[25] W. Xu, K. Song, S. Ma, B. Gao, Y. Chiu, and Y. K. Lee, “Theoretical and experimental investigations of thermoresistive micro calorimetric flow sensors fabricated by CMOS MEMS technology,” *J. Microelectromech. Syst.*, vol. 25, pp. 954–962, 2016.

[26] J. M. Tsai *et al.*, “Versatile CMOS-MEMS integrated piezoelectric platform,” in *Proc. IEEE Transducers*, Anchorage, AK, USA, Jun. 21–25, 2015, pp. 2248–2251.

[27] Z. Dong, J. Chen, Y. Qin, M. Qin, and Q. Huang, “Fabrication of a micromachined two-dimensional wind sensor by Au–Au wafer bonding technology,” *J. Microelectromech. Syst.*, vol. 21, pp. 467–475, 2012.

[28] L. V. King, “On the convection of heat from small cylinders in a stream of fluid: Determination of the convection constants of small platinum wires, with applications to hot-wire anemometry,” *Philosoph. Trans. Roy. Soc. London A*, vol. 90, pp. 563–570, 1914.

[29] W. Xu, “Micromachined thermal flow sensor based on CMOS MEMS technology,” Ph.D. dissertation, Dept. Mech. Aerosp. Eng., Hong Kong Univ. Sci. Technol., Hong Kong, 2017.

[30] A. Perry and G. Morrison, “A study of the constant-temperature hot-wire anemometer,” *J. Fluid Mech.*, vol. 47, no. 3, pp. 577–599, 1971.